Thermochimica Acta, 65 (1983) 269–284
Elsevier Science Publishers B.V., Amsterdam – Printed in The Netherlands

EFFECTS OF EXPERIMENTAL VARIABLES ON THE DETERMINATION OF KINETIC PARAMETERS WITH DIFFERENTIAL SCANNING CALORIMETRY. II. CALCULATION PROCEDURE OF FREEMAN AND CARROLL

ADRIANUS A. VAN DOOREN *

Department of Pharmaceutical Development, Duphar B.V., 1381 CP Weesp (The Netherlands)

BERND W. MÜLLER **

Laboratorium voor Pharmaceutische Technologie, Rijksuniversiteit, Groningen (The Netherlands)

(Received 17 December 1982)

ABSTRACT

The effects of sample mass, heating rate and particle size on the determination of reaction order, activation energy and pre-exponential factor with the calculation procedure of Freeman and Carroll in differential scanning calorimetry was studied with factorial designs. Sodium bicarbonate, three organic hydrates (potassium oxalate hydrate, mercaptopurine hydrate, and sodium citrate dihydrate) and two substances giving solid–solid transformations (potassium nitrate and hexamethylbenzene) were studied. It was found that the extent of these effects depended on the nature of the decomposition and on the evaluated section of the transition peak. It was not justified to use data from the complete peak in the calculation, as different processes contribute to the total solid-state reactions. Arrhenius plots with such data were curved.

In the initial section of the peak heat transport is the main process; high values of the kinetic parameters are then obtained. Lower values, with smaller error, were found for the middle section where mass transport is the predominant process.

Narrow peaks gave rise to very high activation energies and large error. Even negative reaction orders were then found which are indicative of the explosive character of the transition. As the kinetic parameters differ considerably during the peak, it is not justified to attribute any physical meaning to them.

INTRODUCTION

In an earlier paper, we discussed the effects of particle size and sample mass on the determination of kinetic parameters by means of Ozawa and

* To whom correspondence should be addressed.
** Present address: Lehrstuhl für Pharmazeutische Technologie, Christian Albrechts Universität, Kiel (B.R.D.)

0040-6031/83/$03.00

Kissinger plotting [1]. As model substances we used sodium bicarbonate, evolving CO_2, three compounds that lose water of hydration, and two compounds showing polymorphic transitions. In this paper we present the results calculated on the same curves by means of the method of Freeman and Carroll [2]. In this calculation procedure it is assumed that (a) the order of the reaction is the same during the complete transition, (b) the temperature in the sample bed is the same, and (c) there is no effect of atmosphere. Although it has been argued that these assumptions are generally invalid [3], many examples of this method are given in the literature [4,5]. It has also been applied to the Mettler TA 2000 DSC system where normally 5–10 data points are used for calculation [6,7].

It is known that activation energies of solid-state reactions have no physical meaning and it has even been stated that in these reactions an activated state does not occur [8]. However, as Garn [9] pointed out, the need to transport energy permits a calculated activation energy to be obtained. Similar considerations apply to the pre-exponential factor, which is the reaction rate at infinite temperature. This is considered to describe the initial state of the sample [10].

EXPERIMENTAL

A description of the test substances, equipment, calibration and study design is given in part I of this series [1]. In the Freeman and Carroll procedure, the temperatures and residual peak areas were calculated at seven points of the peak (Fig. 1). Reaction orders were obtained from the following four sets of three data points:

(a) mean values of orders over points 1–4–7, 2–4–6, 3–4–5 (complete curve);

(b) over points 1–2–3 (initial part of the curve);

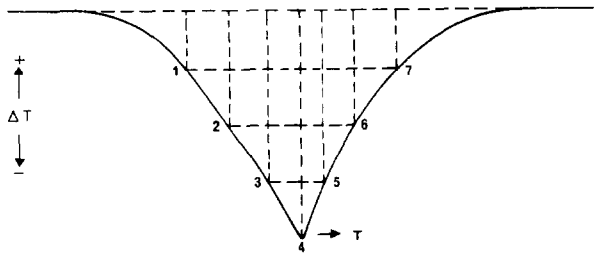

Fig. 1. Data points used in the calculation of kinetic parameters. 1–2–3, Initial section; 3–4–5, middle section; 5–6–7, final section.

(c) over points 3–4–5 (middle part of the curve);
(d) over points 5–6–7 (final part of the curve).

With the reaction orders the reaction rates at any point were calculated, and their natural logarithms were plotted against the reciprocal of the absolute temperature at that point. The activation energy (E_a) was found from the slope of the plot, and the pre-exponential factor from the ordinate intercept.

RESULTS AND DISCUSSION

The reaction orders calculated from different parts of the curve varied considerably. For example, Table 1 gives the reaction orders of sodium bicarbonate, where the data points are designated as in Fig. 1. In the derivation of the Freeman–Carroll procedure, it is assumed that the order of the reaction remains constant during the transition [3]. As this assumption clearly does not hold, it is not justified to calculate an activation energy from the complete curve. It is also evident that the Freeman–Carroll plot of the natural logarithm of the reaction rates (determined with an overall reaction order) against $1/T$ gives a curved line (Fig. 2) from which the activation energy and the pre-exponential factor cannot be determined according to a linear model.

The conversion curves from the corresponding DSC peaks (Fig. 3) make it clear that the reaction consists of three periods: an induction period, an acceleration period, and a decay period. Generally, it can be assumed that nucleation is the predominant factor in the induction period while nucleus

TABLE 1

Reaction orders of $NaHCO_3$ for different sets of data points

Heating rate (K sec^{-1})	Calculated from points [a]	Mass (mg)					
		1	2	4	6	8	Mean
0.04	1–3	5.92	3.92	3.27	1.19	1.10	3.08
	3–5	0.36	0.33	0.37	0.32	0.28	0.33
	5–7	−1.14	0.94	0.86	2.49	2.36	1.56
0.08	1–3	4.04	2.94	1.66	1.39	0.95	2.20
	3–5	0.32	0.35	0.32	0.33	0.29	0.32
	5–7	1.10	1.16	1.46	1.77	2.29	1.56
0.16	1–3	3.53	2.97	1.75	1.05	0.92	2.05
	3–5	0.34	0.34	0.34	0.30	0.30	0.33
	5–7	1.28	1.26	1.55	1.46	1.58	1.43

[a] See Fig. 1.

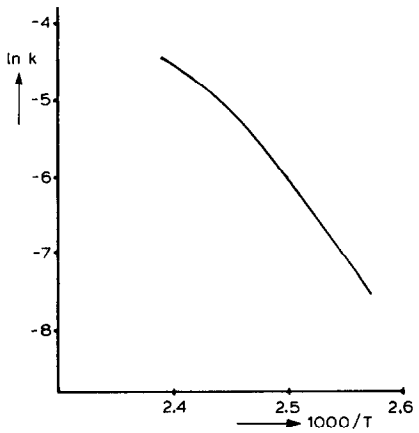

Fig. 2. Freeman–Carroll plot of ln k vs. $1/T$ for $NaHCO_3$ determined over the complete DSC peak.

growth and branching of nuclei is the determining process during the acceleration period. The decrease of branching by contact between the various branched nuclei ('break-off') would correspond with the decay period.

To compare the effects of experimental variables, it may therefore be more interesting to use the data calculated from different parts of the curve. However, for the acceleration and decay periods it is, of course, useless to speak of an 'activation energy'. It may be better to use the term 'temperature coefficient of the reaction' [3].

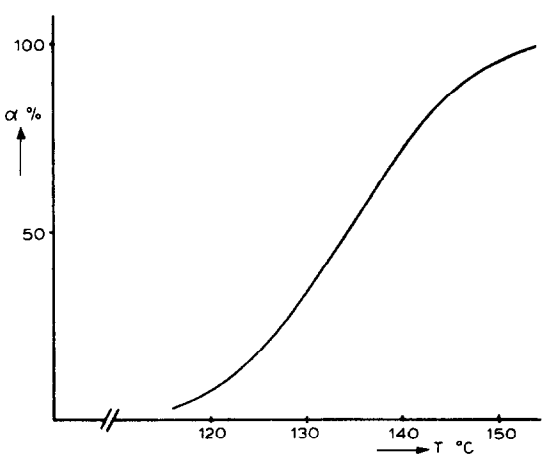

Fig. 3. Conversion curve (α vs. temperature) determined from a DSC peak of $NaHCO_3$.

Sodium bicarbonate

Table 2 shows the effects of heating rate and particle size distribution on the reaction orders determined over the complete peak. The coefficient of variation (CV) of the determination is approximately 25% and Table 2 shows that the value of the reaction order for the milled, small and complete size samples is 1.2 whereas for the mean size sample it is 1.0 and for the large particles it is 0.9.

Statistical analysis shows a significant interaction ($P = 0.01$) between heating rate and particle size distribution. This is because for large particles the reaction order increases with heating rate (β), whereas for the other sizes it generally increases if β increases from 0.01 to 0.02 or 0.04 K sec^{-1}, then it decreases for the intermediate heating rates, and it increases again if β changes from 0.16 to 0.32 K sec^{-1}. Only in the case of comminuted particles does the reaction order not change if β changes from 0.16 to 0.32 K sec^{-1}. In solid-state reactions, the reaction order does not have a physical meaning [3]. However, the mathematical calculation shows that a high order corresponds with a high reaction rate.

As we discussed in an earlier paper [11], an increase in heating rate or particle size leads to greater thermal lags within the sample powder bed. This leads to wider peaks and smaller instantaneous heat flows and, thus, smaller peak heights. In the Freeman–Carroll procedure this results in lower reaction orders and reaction rates. However, if the heating rate is too high, superheating may occur in the powder bed, leading to an increase in reaction rate. On the other hand, if the heating rate is extremely low (< 1 K min^{-1}) the energy input per unit time into the sample is very low, which leads to a considerable 'self-cooling' effect in a sample undergoing an endothermic reaction. Moreover, at such low heating rates equilibration may occur, also

TABLE 2

Mean reaction orders on complete peaks of $NaHCO_3$

Heating rate β (K sec^{-1})	Particle size					
	Milled	Small	Medium	Large	Complete spectrum	Mean
0.01	1.08	1.32	0.91	0.76	1.14	1.04
0.02	1.16	1.32	1.04	0.84	1.30	1.13
0.04	1.34	1.14	1.01	0.84	1.33	1.13
0.08	1.18	1.09	0.98	0.90	1.21	1.07
0.16	1.21	1.05	1.00	0.94	1.10	1.06
0.32	1.21	1.19	1.15	1.11	1.14	1.16
Mean	1.20	1.19	1.02	0.90	1.20	1.10

lowering the reaction rate. At heating rates < 1 K min^{-1}, the reaction order is therefore very low.

In larger particles, this self-cooling effect is more predominant than with smaller ones, which means that to overcome this effect the heating rate should be higher for larger particles. The decrease of reaction order due to greater thermal lags is so counteracted and the result is an increase in reaction order for large particles.

Effects of sample mass on the overall reaction orders were also observed. In general, a higher sample mass leads to greater thermal lags and self-cooling effects, and so to wider peaks and smaller reaction orders. However, for sample sizes as low as 1 mg the overall reaction order was found to be lower than expected. This is presumably due to a greater inaccuracy in the determination as the thermal effect is smaller.

It should be noted that the effects of thermal resistance in the powder bed are only relevant for the Mettler DSC apparatus, where the sample holder is based on a thermal insulator and where heat transfer is partly accomplished by convection of the furnace atmosphere.

Comparison of the reaction orders calculated for the different parts of the curve (Table 1) shows that they change considerably throughout the reaction. In the initial part of the curve, corresponding with the descending part of the peak (points 1–3 where $0.03 < \alpha < 0.30$) the reaction order is generally between 2 and 6. In the middle part, corresponding with the straight part of the conversion curve (Fig. 2), where $0.30 < \alpha < 0.85$ the reaction order is 0.3–0.4. In the last part of the curve, corresponding with the ascending line of the peak, where $0.85 < \alpha < 0.97$, the order is 1–2. To explain such behaviour it may be argued that in the first part of the curve, heat transport is the main process (corresponding with high rates), and in the following sections it is mainly mass transport (gas molecules leaving the surface) [12]. We believe that in the last part of the peak the temperatures in the sample become so high that the rate of mass transport is increased. The rates in the middle part of the curve are lower because gas molecules building up a pressure in the surroundings of the sample particles suppress the reaction rate.

A decrease of reaction order by increase of sample mass, as was observed for the mean overall orders, is only shown in the first part of the peak. This clearly comes from the self-cooling properties of the sample as the temperatures are not yet high enough. In the middle part of the curve, the rates do not change with sample mass, and in the final part the reaction rates actually increase with sample mass (especially at low heating rates). Apparently, in the latter parts of the curves the above-mentioned influences of self-insulating properties of large masses, causing greater thermal lags, disappear, and the relatively large energetic effects of the mass transport of CO_2 molecules leaving the surface lead to increases in reaction rates. Another possible explanation is that at larger sample sizes so much CO_2 evolves that the

diffusion of this gas from the (pierced) sample holder is much greater than for small samples, which would lead to a lower CO_2 pressure in the immediate surroundings of the particles. The activation energies and pre-exponential factors determined over the initial period are extremely high (Table 3), as were the reaction orders.

A similar decrease with increasing sample mass as for the reaction orders was observed for E_a and ln Z. Their values in the linear section of the conversion curve (points 3–4–5 in Fig. 1) are much lower than those in the initial period. If the activation energies over this section are calculated using the overall mean reaction order, values of 100–140 kJ mole^{-1} are obtained, but if the orders applicable for this section (0.30–0.37) are used, the activation energies are approximately 70–85 kJ mole^{-1} (CV 5.7%). The latter values correspond reasonably well with the data given by Subramanian et al. [13].

There is a significant effect of sample mass on the E_a and ln Z calculated from the linear section of the conversion curve ($P = 0.01$). However, in contrast to the effects on the initial part of the curve, this effect is caused by the lower values for the lower masses. It can be explained in the same way as the influence of mass on the different reaction orders.

Effects of heating rates and particle sizes on activation energy are shown in Table 4. The values for the initial section are extremely high and have been determined with a coefficient of variation of 23%. In general, the activation energy decreases with heating rate and the comminuted particles also have a lower E_a than the other fractions, although due to large variations statistical significance was not attained. The same applies to the corresponding pre-exponential factors.

Potential nucleation sites have different energy states. Due to milling, particle surfaces are broken. This leads to an increase in the energy state. Therefore, in comminuted particles, the increment in energy required to

TABLE 3

Effects of sample masses on kinetic parameters obtained from different parts of $NaHCO_3$ curves [a]

Mass (mg)	E_a (kJ mole^{-1})		ln Z	
	Initial section	Middle section	Initial section	Middle section
1	263.8	71.5	89.7	13.3
2	249.8	75.0	80.2	14.9
3	202.3	83.6	61.0	16.5
4	158.1	85.0	42.6	16.7
5	146.5	83.0	38.0	15.3

[a] The values presented were calculated over all heating rates.

TABLE 4

Activation energies of sodium bicarbonate decomposition

Heating rate (K sec^{-1})	Section of curve [a]	Particle size				
		Comminuted	Small	Medium	Large	Complete spectrum
0.01	Initial section	289.9	447.5	380.1	414.4	360.3
	Middle section	96.9	98.4	68.0	61.9	59.6
0.02	Initial section	253.7	494.8	418.9	355.1	267.0
	Middle section	96.4	97.0	81.0	70.4	76.2
0.04	Initial section	246.1	415.5	364.3	223.3	385.8
	Middle section	87.7	90.8	81.0	77.2	73.6
0.08	Initial section	244.3	355.1	373.5	226.9	337.0
	Middle section	83.7	87.3	85.9	80.1	70.0
0.16	Initial section	234.9	348.6	309.7	185.8	234.2
	Middle section	77.8	84.3	85.8	79.1	67.6
0.32	Initial section	198.0	317.8	325.8	295.3	304.4
	Middle section	70.8	85.2	82.5	79.2	64.1

[a] See Fig. 1.

reach the activated state is smaller than in more perfect crystals [14]. A higher energy input per unit time (i.e. a higher heating rate) may also increase the probability of reaching the activated state or, in other words, decreases activation energy.

The effects of particle size and heating rate on the E_a from the linear part of the conversion curve (middle section of the DSC peak) are different (Table 4): increase in heating rate generally decreases the E_a for the comminuted and small particles. For the medium and large particle samples, a higher heating rate increases E_a. The effect of heating rate on the sample with complete size spectrum cannot be determined clearly due to its large coefficient of variation. The main effect of particle size in the middle region of the DSC curve appears to be that an increase in size leads to a decrease in E_a.

The linear parts of the curves for milled and small particles are steeper than the same parts of the curves of the larger particles. This corresponds with a steeper line in the plot of ln k vs. $1/T$, i.e. a higher temperature coefficient of this part of the reaction and a higher pre-exponential factor. If the heating rate is increased, the total peak becomes wider and for the milled and small particles this means that the temperature differences between given conversions become greater and the ln k vs. $1/T$ plot less steep, leading to a decrease of E_a at higher heating rates. Apparently, the effect is

reversed for the larger particles: the shorter transition times at higher heating rates lead to steeper lines and higher E_a values.

Potassium oxalate monohydrate

The mean reaction order calculated over the complete peak in the experiment where heating rate and particle size were varied was 0.67 (CV 24%). When heating rate and sample size were varied, the mean overall reaction order was 0.60 (CV 3.5%). As for $NaHCO_3$, an increase with increasing heating rate and a decrease (though small) with increasing sample mass were observed. Only the value for the highest sample size was somewhat higher than expected. This was particularly due to a very high value at the highest heating rate.

The reaction orders calculated from different parts of the curves can be compared in Table 5. The reaction orders for the initial part of the curve, where heat transport is the main process, are much higher than in the middle

TABLE 5

Reaction orders of potassium oxalate dehydration

Heating rate ($K\ sec^{-1}$)	Data points of curve [a]	Particle size					
		Milled	Small	Medium	Large	Complete size spectrum	Mean
0.01	1–3	2.56	5.07	2.73	2.11	3.20	3.14
	3–5	0.32	0.22	0.23	0.25	0.21	0.25
	5–7	0.66	1.70	1.26	0.86	0.84	1.06
0.02	1–3	1.84	2.62	2.23	2.59	2.00	2.26
	3–5	0.25	0.23	0.22	0.24	0.24	0.24
	5–7	1.44	1.07	1.35	1.16	0.81	1.17
0.04	1–3	1.03	1.16	1.11	0.97	1.61	1.18
	3–5	0.25	0.22	0.28	0.24	0.28	0.24
	5–7	1.83	1.27	1.94	1.70	1.76	1.70
0.08	1–3	0.82	0.90	1.28	0.80	0.96	0.95
	3–5	0.26	0.25	0.24	0.28	0.25	0.25
	5–7	2.00	2.39	14.80	1.42	6.42	5.41
0.16	1–3	0.81	1.22	0.75	0.80	0.72	0.86
	3–5	0.33	0.30	0.31	0.34	0.29	0.31
	5–7	2.28	1.99	3.39	5.62	1.56	2.97
0.32	1–3	0.64	0.56	0.71	0.48	0.57	0.59
	3–5	0.36	0.41	0.39	0.39	0.39	0.39
	5–7	7.91	1.51	2.79	1.50	1.42	3.03

[a] See Fig. 1.

part (which corresponds with the linear section in the conversion curve). In the last part of the curve ($0.85 < \alpha < 0.95$) the temperatures are so high that the rate of mass transport is increased and higher reaction orders are again obtained. The variation in the values obtained for this section is very large, especially at rates $\geqslant 0.08$ K sec^{-1}.

One of the reasons for the very low reaction orders in the middle part of the curves may be the dissolution of some potassium oxalate crystals in their released water of hydration. This process is presumably endothermic, will therefore require energy, and lead to a decrease in sample temperature. In the later stage, recrystallisation will occur together with evaporation of the water of hydration, the rates of these processes depending on the evaporation through the powder bed.

The evaporation therefore depends on many factors like porosity, particle size (distribution) and packing. These factors may even change throughout the course of the reaction, which explains the large variations in the reaction orders. The rates of recrystallisation and evaporation are higher with higher heating rates. Therefore, the reaction orders determined over the final parts of the curve increase with increasing heating rate. Furthermore, Table 5 shows that at high heating rates ($\geqslant 0.16$ K sec^{-1}) the orders in the middle part of the curve are also higher, which may be because at these rates recrystallisation and evaporation already occur in the middle parts of the curves.

For the initial part of the curve we observed lower reaction orders with higher heating rates. Assuming that in this curve section heat transport is the main process, the increases in thermal lags and widening of the peaks at higher rates may account for this observation. These thermal lags, which are greater in large particle samples, may also be the cause of the decrease in reaction order when particle size is increased. At low heating rates, the reaction order for the comminuted fractions is, however, higher than those of the small sized samples; the cause may be that dissolution already occurs in the initial part of the curve, particularly at lower heating rates. In the first section of the curve, the reaction orders decrease with increasing sample masses and heating rates, corresponding with increasing thermal lags within the samples. In the middle sections, again an increase in reaction orders with heating rate ($P = 0.01$) was observed at rates > 0.08 K sec^{-1} and for the final sections, the intricate processes of water evolution, crystal dissolution, recrystallisation and evaporation, which are dependent on both sample mass and heating rate, may account for the significant interaction between these experimental variables.

The determination of the effects of heating rates and sample sizes on the activation energy for the initial part of the curve had a coefficient of variation of 6.0%. The mean E_a was 120.6 kJ mole^{-1}. A similar decrease in E_a with increasing sample mass was found as for sodium bicarbonate. If for the same experiments the activation energies were determined from the

linear sections of the conversion curve, the CV was 4.7% (with a mean value for E_a of 95.6 kJ mole^{-1}) and a slight but significant (at the 1% level) interaction between sample mass and heating rate was observed. This was because at low masses E_a decreased with increasing heating rates, whereas at high rates the opposite occurred. If heating rates and particle sizes were varied, the activation energies and pre-exponential factors for the initial sections of the curves were determined with high standard deviations (approximately 21%) and they had very high values (213 kJ mole^{-1} and 67.6, respectively). At low heating rates and particle sizes, values for the activation energy as high as 500 kJ mole^{-1} were obtained. Increase in heating rate and particle size decreased the responses, which is explained similarly as the effects on reaction orders.

In the experiment with different heating rates and particle sizes, the mean energy calculated for the middle part of the curve was 96.3 kJ mole^{-1} (CV 5.3%), if the values for the comminuted fraction (121 kJ mole^{-1}) and heating rate 0.01 K sec^{-1} (126 kJ mole^{-1}) were omitted.

Mercaptopurine hydrate

The reaction order of the dehydration of mercaptopurine hydrate determined over the complete peak decreases if the heating rate is increased from 0.01 to 0.08 K sec^{-1}, but increases again if the heating rate is increased still further. The first decrease is explained by the greater thermal lags and widening of peaks at higher rates, but at rates $\geqslant 0.08$ K sec^{-1} superheating increases the reaction orders. There is an interesting difference in reaction order between the complete size spectrum sample ($n = 1.00$) and the comminuted sample ($n = 0.60$). Such a difference is also observed in the initial part of the curve ($n = 1.38$ for the complete spectrum and $n = 0.90$ for the comminuted sample) and in the middle section (where $n = 0.39$ and 0.27, respectively). It should be noted that the mean particle sizes of the two samples (15 and 5 μm, respectively) do not differ much so different thermal lags and self-cooling effects due to size differences are rather unlikely. Comminution of mercaptopurine hydrate leads to increase in the number of cracks and strains and thus to an enlargement of the particle surface. Not only would the probability of nucleation then be increased, but also the dissolution of the particles into the released water of hydration. This would lead to lower apparent reaction orders, apparently even in the first part of the transition. Due to rather large standard deviations, no differences in activation energies or pre-exponential factors between the milled and complete size spectrum samples were observed.

Table 6 presents the kinetic parameters for the initial parts of the curves when heating rate and sample mass were varied. Interestingly, the reaction order has a negative value at high heating rates and high sample masses. Theoretically this means that the reaction is autocatalytic. Negative reaction

TABLE 6

Kinetic parameters for initial section of mercaptopurine dehydration curve (complete size spectrum)

Heating rate (K sec^{-1})	Parameter	Mass (mg)				
		1	2	4	6	8
0.04	Reaction order	1.95	0.97	0.67	0.47	0.35
	E_a (kJ $mole^{-1}$)	190.7	139.9	123.6	112.7	109.2
	ln Z	54.62	34.07	27.14	22.68	20.89
0.08	Reaction order	1.56	0.69	0.38	−0.07	−0.28
	E_a (kJ $mole^{-1}$)	154.1	119.1	107.8	96.5	93.3
	ln Z	41.59	26.39	21.12	15.21	13.04
0.16	Reaction order	0.90	0.52	−1.29	−2.33	−2.13
	E_a (kJ $mole^{-1}$)	119.2	109.7	64.9	53.7	109.0
	ln Z	27.93	22.88	2.11	0.51	7.71

orders calculated with the Freeman–Carroll method may be caused by large variations in the data point coordinates, small temperature differences between the data points (narrow but steep and sharp peaks), but also by a dramatic acceleration of the reactions due to different processes in the powder bed, like superheating, nucleus growth and turbulent diffusion of gas from the particle surfaces.

Table 6 also shows the decrease of activation energy and pre-exponential factor with increasing sample mass and heating rate. This can be explained in the same way as for sodium bicarbonate and potassium oxalate. Only at the highest mass and heating rate, is the activation energy higher than expected.

Sodium citrate dihydrate

Sodium citrate dihydrate loses its water over a narrower temperature interval than potassium oxalate hydrate and mercaptopurine hydrate. As the temperature differences during the peak are, therefore, much smaller, the error in the determination of reaction order is much greater than for the other two dehydrations. Averaging and statistical evaluation was therefore not feasible. At high heating rates, we found negative values for the reaction orders over the initial parts of the peaks. This may be caused by slight errors in the temperature determinations, but we also believe that at these heating rates the dehydration is autocatalytic: superheating and turbulent diffusion can lead to an explosive reaction. The reaction order over the middle parts of the peaks increased with increasing heating rate, as is shown in Table 7. This can be explained from the increase in superheating. The activation energies

TABLE 7

Effects of heating rates on kinetic parameters for middle part of sodium citrate dehydration curve [a]

β (K sec^{-1})	Reaction order	E_a (kJ mole^{-1})	ln Z
0.01	0.59	843	231
0.02	0.36	817	222
0.04	0.37	748	201
0.08	0.39	781	210
0.16	0.44	621	165
0.32	0.53	492	129

[a] Values for comminuted fraction excluded.

and pre-exponential factors are subject to large experimental error (16%). Table 7 shows their very high values, generally decreasing with heating rate. These values indicate the explosive character of the reaction.

At low heating rates the comminuted samples did not show a dehydration peak in the temperature range examined. This corresponds with the findings of Maeda et al. [15], who found that sharp dehydration peaks of organic materials were not necessarily caused by grinding, but rather by not grinding them. They assumed that a rise in temperature during milling led to premature dehydration.

Potassium nitrate

The II–I polymorphic transition of potassium nitrate is represented by a very sharp and narrow peak on the DSC curve. Even at low heating rates the transitions occur so fast that reaction orders over the complete peak or its first part can only be obtained with extremely large variations. In the middle parts of the curves, the mean reaction order was 0.56. It increased with heating rate due to superheating, and the corresponding activation energies and pre-exponential factors decreased with increasing heating rate: at $\beta =$ 0.01 K sec^{-1}, $E_a = 2715$ kJ mole^{-1} and ln $Z = 804$; at $\beta = 0.32$ K sec^{-1}, $E_a = 488$ kJ mole^{-1} and ln $Z = 140$.

The values of the kinetic parameters decrease with increasing sample mass. Higher masses make the temperature differences between the data points greater, which leads to lower activation energies. The kinetic parameters averaged for different particle sizes are given in Table 8. E_a and Z are generally extremely high, but for the comminuted particles they are lower than for the other fractions, presumably due to their lower degree of perfection, or because a small amount already transformed during the comminution process.

TABLE 8

Kinetic parameters for middle curve sections of potassium nitrate and hexamethylbenzene

Substance	Parameter	Particle size				
		Comminuted	Small	Medium	Large	Complete size spectrum
KNO_3	Reaction order	0.54	0.63	0.55	0.52	0.54
	E_a (kJ mole^{-1})	989	1706	1836	1364	1929
	ln Z	289	503	542	401	569
Hexamethyl benzene	Reaction order	0.51	0.65	0.58	0.79	0.76
	E_a (kJ mole^{-1})	1055	1140	1157	4314	3753
	ln Z	323	350	355	1344	1167

Hexamethylbenzene

The enthalpy change corresponding with the solid–solid transition of hexamethylbenzene is very low (~ 9.4 J g^{-1}) and the peak occurs over a very small temperature range (111–114°C). The accuracy of the determination of temperatures and conversions at the data points is therefore low, which leads to very low reproducibility. Some results are presented in Table 8. This Table shows that the activation energy and pre-exponential factor are even higher than those of the KNO_3 transition, and again the comminuted fraction showed smaller values. Since the mass fraction of large particles in the complete size spectrum is very high, the values for the complete size spectrum correspond very well with those of the large particle fraction. Activation energies and pre-exponential factors again decrease with heating rate.

SUMMARY AND CONCLUSIONS

Factorial experiments were carried out to investigate the effects of sample size, particle size and heating rate on the determination of kinetic parameters with Freeman and Carroll plots. A commercial heat-flux DSC apparatus was used and as models for solid-state reactions the following substances were studied: sodium bicarbonate (evolution of CO_2); potassium oxalate monohydrate, 6-mercaptopurine monohydrate and sodium citrate dihydrate (dehydrations), potassium nitrate and hexamethylbenzene (solid–solid transformations).

The Freeman and Carroll plots with data points from the complete decomposition peaks were curved, so, in order to evaluate effects of the

operational variables, the reaction orders were calculated over different parts of the peaks. These points largely correspond to an induction period, acceleration period, and a decay period in the conversion curve. In the case of sodium bicarbonate, heating rates, sample masses and particle sizes affected the reaction orders significantly. This was explained either by thermal lags and self-cooling effects in large particles and high sample masses, which lead to decreases in apparent reaction or by superheating which may occur at high heating rates. Such phenomena may occur because of the construction of the DSC furnace. Activation energies and pre-exponential factors determined were very high in the initial period, but in the middle region they were much lower: E_a values of 70–80 kJ mole^{-1} were then obtained with ln Z between 13 and 16 and reaction orders of 0.30–0.37. In the middle region of the curve an increase in size led to a decrease in activation energy.

The overall mean reaction order for the dehydration of potassium oxalate monohydrate was 0.60–0.67. Again, different values of reaction orders for the different regions were obtained. The high values in the initial part were assumed to be due to heat transport, whereas mass transport would mainly occur in the later stages. In the middle part, corresponding with the linear section in the conversion curve, the reaction orders were very low, which may be due to the dissolution of some potassium oxalate crystals in their released water of hydration. In the final section, recrystallisation will occur together with evaporation of the water. The experimental variables affected all kinetic parameters, but the extent of these effects depended on the section of the curve that was evaluated.

For mercaptopurine hydrate, the reaction order differed between the complete size spectrum sample ($n = 1.00$) and the comminuted sample ($n = 0.60$). At very high heating rates and high sample masses the reaction order had a negative value. This indicates that different processes in the powder bed, such as superheating, nucleus growth and turbulent diffusion of gas from the particle surface, lead to autocatalytic reactions.

Sodium citrate dihydrate loses its water over a much narrower temperature interval than the other hydrates. This correlates with very high values of the kinetic parameters, and large errors which impair statistical analysis. At high heating rates, we also observed negative reaction orders which indicate the explosive character of sodium citrate dehydration. At low heating rates the comminuted samples did not show a dehydration peak. The narrow peak of the transition of potassium nitrate also led to large experimental error. Only for the middle section of the curve were 'acceptable' values of the reaction order (mean 0.56) obtained. The corresponding activation energies were extremely high (mean 1565 kJ mole^{-1}). For hexamethylbenzene the same applied, the values for the kinetic parameters being even higher. The kinetic parameters for the polymorphic transition of potassium nitrate decreased with increasing sample mass. Again, effects of particle size and heating rate were also observed.

In conclusion, sample mass, particle size and heating rate affect the values of the reaction order, activation energy and pre-exponential factor obtained with the procedure of Freeman and Carroll. The extent of these effects depends primarily on the nature of the decomposition, but also on the evaluated section of the transition peak. Many of these effects could be explained on the basis of the existence of thermal lags within the powder beds. The construction of the DSC furnace also plays a role. It is not justified to use the complete peak in the determination, as different processes contribute to the total solid-state reactions. The Freeman–Carroll plot with data points of the complete peak, is curved which does not allow calculation of activation energies. In the initial section of the peak heat transport is the main process. High values of kinetic parameters are then obtained. Lower values, with smaller errors, were found for the middle section where mass transport is the main process. Sharp and narrow peaks gave rise to very high values of activation energy and large experimental error. Even negative reaction orders were found, which are indicative of the explosive character of the transition under study. Arrhenius plots (and extrapolation of reaction rates to room temperature) are not valid in explosive reactions. As the kinetic parameters differ so largely during the peak, it is not justified to attribute any physical meaning to the kinetic parameters obtained with the Freeman and Carroll method.

ACKNOWLEDGEMENTS

We thank Dr. P. van Bemmel (Duphar B.V., Weesp, The Netherlands), for statistical analysis and helpful discussions, and Messrs J.W. Van der Kuy and S.J.W. Vroklage (Duphar B.V., Weesp, The Netherlands), for doing part of the experimental work and drawing the figures.

REFERENCES

1 A.A. van Dooren and B.W. Müller, Thermochim. Acta, 65 (1983) 257.
2 E.S. Freeman and B. Carroll, J. Phys. Chem., 62 (1958), 394.
3 P.D. Garn, Crit. Rev. Anal. Chem., Sept. (1972) 65.
4 B. Carroll and E.P. Manche, Thermochim. Acta, 3 (1972) 449.
5 E. Segal and D. Fatu, J. Therm. Anal., 9 (1976) 65.
6 V. Schlichenmaier and G. Widmann, Proc. Symp. Therm. Anal., Salford, 1976, p. 77.
7 V. Schlichenmaier and G. Widmann, Thermochim. Acta, 21 (1977) 39.
8 J. Simon, J. Therm. Anal., 5 (1973) 271.
9 P.D. Garn, J. Therm. Anal., 13 (1978) 581.
10 J. Sestak and G. Berggren, Thermochim. Acta, 3 (1971) 1.
11 A.A. van Dooren and B.W. Müller, Thermochim. Acta, 54 (1982) 115.
12 J. Simon, E. Buzagh-Gere and S. Gal, Proc. 3rd Int. Conf. Therm. Anal., 1972, p. 393.
13 K.S. Subramanian, T.P. Radhakrishnan and A.K. Sundaram, J. Therm. Anal., 4 (1972) 89.
14 R. Huettenrauch, Acta Pharm. Tech. Suppl., 6 (1978) 55.
15 Y. Maeda, T. Azumi and S. Takashima, Nippon Kagaku Zasshi, 85 (1964) 863.